The Effect of Solar Radiation on the Ampacity of an Underground Cable with XLPE Insulation


Dardan Klimenta
University of Priština in Kosovska Mitrovica


Miroljub Jevtic
University of Pristina


Bojan Perovic
University of Pristina

The Effect of Solar Radiation on the Ampacity of an Underground Cable with XLPE Insulation

Dardan Klimenta[1], Miroljub Jevtić[2], Jelena Klimenta[3], Bojan Perović[4]

[1]University of Priština in Kosovska Mitrovica, Kosovska Mitrovica, Serbia, dardan.klimenta@pr.ac.rs
[2]University of Priština in Kosovska Mitrovica, Kosovska Mitrovica, Serbia, miroljub.jevtic@pr.ac.rs
[3]Independent Consultant in the Field of Urban and Spatial Planning, Niš, Serbia, klimenta.jelena@gmail.com
[4]University of Priština in Kosovska Mitrovica, Kosovska Mitrovica, Serbia, bojan.perovic@pr.ac.rs

Abstract— **The main purpose of this paper is to quantify the thermal effect of solar radiation on the ampacity of a low voltage underground cable with cross-linked polyethylene (XLPE) insulation. The quantification was performed for different laying depths of the cable, different colors of the upper surface of the pavement above the cable, different dimensions of the cable bedding, various load currents, various solar irradiances and different periods of the year. Simulation results were obtained using the finite element method in COMSOL and were compared with the corresponding experimental data. It was found that the ampacity of the XLPE-cable installed at a standard depth of 0.7 m can be increased up to 25.6 % in summer and up to 10.2 % in winter compared to the corresponding base cases.**

Keywords— ampacity, finite element method (FEM), heat transfer, power cable, solar radiation

I. INTRODUCTION

The thermal effect of the Sun on underground power cables is becoming more important with the overall average rise in temperature of the Earth's surface (and atmosphere) due to climate change. During the summer months, the electricity consumption for air conditioning of residential and business premises is growing with the increase in ambient temperature. Accordingly, solar heating of soils reduces the ampacity of underground cable lines, and the increase of electricity consumption reduces their power availability. In addition, the thermal effect of the Sun on underground power cables is more pronounced at lower laying depths.

The relevant standards [1-3] do not take into account the thermal effect of the Sun on the ampacity of underground power cables. The number of research papers dealing with this effect is small. All of these papers were written by Klimenta et al. [4-6]. In addition to this, there are researchers who found that solar radiation only affects the cables laid at law depths [7], and researchers who concluded that the effect of the Sun can not be ignored in the case of cables under dynamic loading [8-10].

In this paper, it is shown how the solar heating affects the ampacity of an underground XP-00 4×16 mm^2 0.6/1 kV cable through five different cool pavements at laying depths of 0.4, 0.7 and 1 m where this effect is significant. It is assumed that the three-phase system is balanced, that the heat flux vanishes at a reference distance, and that the 0.5-m-wide cable trench is covered with a cool pavement [4]. The following two cases are considered herein. The first is that the cable is installed in the bedding of standard size. The second is that the cable is installed in the trench completely filled with bedding material. Some simulation results are obtained for known laboratory conditions, for the most unfavourable summer conditions and for the most common winter conditions. The results are generated so that they can be easily compared with the results from [4]. A solid experimental background is provided as well. The XP-00 4×16 mm^2 0.6/1 kV cable considered herein corresponds to the N2XY type in accordance with the DIN VDE standards.

II. Experimental Background

The apparatus, procedure, materials and measurement results that were used as an experimental background for this paper are described in detail in [4-6]. In [4-6], the following experiments were conducted: (i) with pavement made of concrete blocks, (ii) with concrete-pavement coated with acrylic white paint, and (iii) with concrete-pavement coated with acrylic black paint. The reference [4] gives experimental data obtained for the cases where the specified control temperature was fixed at 51, 56 and 61 °C, while the references [5,6] provide data obtained for the cases where this temperature was 66 and 71 °C.

Within the experimental apparatus described in [4-6], the temperature was measured at several points. In this paper, for the purposes of comparing the simulation results with the experimental data from [4-6], the following three points are singled out: A – on the outer surface of the physical model of the cable, B – on the lower surface of the pavement above the physical model of the cable, and C – on the upper surface of the pavement above the physical model of the cable. The temperature at point A was obtained by averaging the measured values at three different points along the physical model of the cable, while the temperatures at points B and C were measured directly. Points A, B, and C are marked within the small-size computational domain, which will be used for numerical simulations in COMSOL. This domain is shown in Fig. 1.

III. 2D FEM-Based Heat Conduction Model

A two-dimensional (2D) FEM-based heat conduction model is created based on the following equation [4]:

$$\frac{\partial}{\partial x}\left(k\frac{\partial T}{\partial x}\right)+\frac{\partial}{\partial y}\left(k\frac{\partial T}{\partial y}\right)+Q_v=0 \qquad (1)$$

where k is the thermal conductivity in W/(m·K); T is the temperature in K; x, y are Cartesian spatial coordinates in m; and Q_v is the volume power of heat sources in W/m^3.

The XP-00 4×16 mm^2 0.6/1 kV cable is modelled by an equivalent construction composed of the four round copper conductors, 0.7-mm-thick core insulations of XLPE, 1.7-mm-thick layer of unvulcanised rubber under the outer sheath and 1.8-mm-thick outer polyvinyl-chloride (PVC) sheath with outer diameters 4.8, 6.2, 18.4 and 22 mm, respectively. In addition, it is assumed that the core insulations and some filling (of unvulcanised rubber) between and around these core insulations represent one object (i.e. block) having the same thermal conductivity as XLPE. Moreover, it is assumed that the 1.7-mm-thick cylindrical layer of unvulcanised rubber has the same thermal conductivity as PVC. The cross-section of this equivalent cable construction is shown in Fig. 1. Fig. 2 presents the large-size computational domain for the case when the cable is laid in the bedding of a standard size 0.5 m × 0.4 m.

In order to increase the mesh density within and around the blocks with heat sources, in both domains, the surface layers of all conductors were modelled by hollow cylinders having thicknesses of 0.4 mm. In addition, in order to ensure the mesh independence, the temperatures of the phase conductors and the load current were tracked. The numbers of nodes and elements were varied from the numbers of nodes and elements corresponding to automatic mesh generation to the numbers of nodes and elements corresponding to mesh refinement, respectively. The differences between the temperatures obtained using different meshes were lower than 0.002 °C for the small-size computational domain and lower than 0.03 °C for the largre-size computational domain. Accordingly, meshes with the number of nodes corresponding to automatic mesh generation were used. Table I deals with the details relating to meshes generated in the considered computational domains, as well as mesh independence tests performed on them.

The volume power of heat sources in the phase conductors with a diameter of d_1=0.0048 m and with a geometric cross-section area of $S'_c = 18.096\cdot 10^{-6}$ m^2 is

$$Q_v = \frac{R_{ac}(T_{cp})}{S'_c}\cdot I^2 \qquad (2)$$

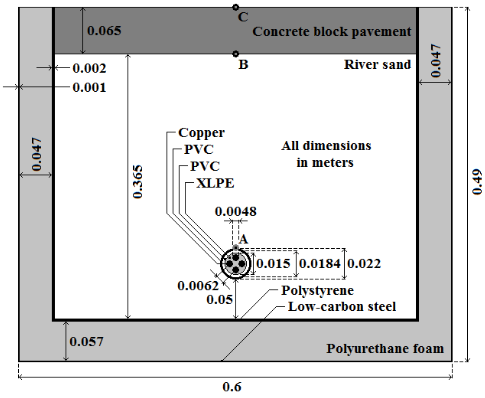

Figure 1. Presentation of the small-size computational domain corresponding to the experimental apparatus.

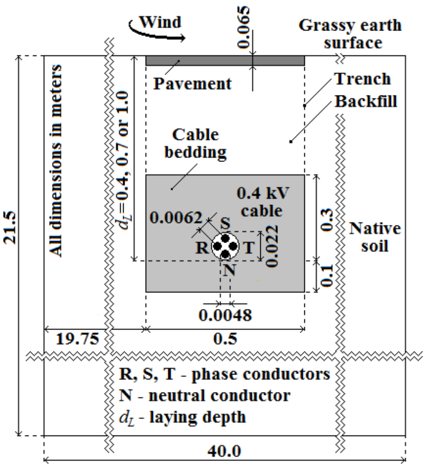

Figure 2. Presentation of the large-size computational domain.

TABLE I. DETAILS ON FINITE ELEMENT MESHES AND MESH INDEPENDENCE TESTS

Domain	Finite element mesh				Temp. differences
	Automatically generated		After refinement		
	No. of nodes	*No. of elements*	*No. of nodes*	*No. of elements*	°C
Small	15146	29101	59392	116404	<0.002
Large, with d_L=0.4 m	1776	3459	7010	13836	<0.03
Large, with d_L=0.7 m	1739	3399	6876	13596	<0.01
Large, with d_L=1 m	1758	3438	6953	13752	<0.02

where $R_{ac}(T_{cp})=R_{20}\cdot(234.5+T_{cp})/254.5=1479.057\cdot10^{-6}$ Ω/m is the a.c. resistance per unit length of a single copper conductor at temperature T_{cp}=90 °C, $R_{20}=1.16\cdot10^{-3}$ Ω/m is the a.c. resistance per unit length of a single copper conductor measured at 20 °C, T_{cp} is the continuously permissible temperature of the XLPE-cable in °C, and I is the cable load current (or cable ampacity when $I=I_{cp}$) in A. In addition, there are no heat sources in the neutral conductor and XLPE insulation [1,4].

From an engineering point of view, it is customary to consider the ampacity I_{cp} for known laboratory conditions, the most unfavourable summer conditions and the most common winter conditions. All these conditions, thermal conductivities of all used materials, boundary conditions and assumptions are the same as in [4]. Therefore, in order to leave more space for the results and discussion, as well as to avoid a repetition of the data, all these details will not be listed here.

IV. RESULTS AND DISCUSSION

A. *Validation of the Model*

Results obtained by simulating the temperature distribution over the small-size computational domain in Fig. 1 for the known laboratory conditions [4] are listed in Table II. For the small-size domain, a sequence of simulations is carried out with white, grey and black pavement surfaces.

When the simulation results from Table II are compared with the corresponding measurement data from [4-6], observations indicating a satisfactory level of accuracy on account of the model used in this paper can be made. The observations are similar to the ones from [4]. The only differences are that the continuously permissible temperature of the considered XLPE-cable is T_{cp}=90 °C and that the results from Table II corresponds to this temperature.

B. *Numerical Results*

In order to generalise the results presented in the previous subsection, the large-size domain in Fig. 2 was created. Temperature distributions over this domain are calculated for the following two cases: I – the cable is installed in the bedding of standard size, and II – the cable is installed in the trench completely filled with bedding. For each of these cases, a sequence of simulations is performed with the laying depth d_L=0.4 m and with cool white coating, acrylic white paint, uncoated concrete blocks, uncoated asphalt and acrylic black paint.

TABLE II. SIMULATION RESULTS OBTAINED FOR THE LABORATORY CONDITIONS

Pavement surface			Temperature							Q_v	*I*
Color	*Absorptivity, α*	*Emissivity, ε*	Phase conductors	Cable's outer surface		Pavement					
						Lower surface		Upper surface			
	–	–		*Sim **	*Diff **	*Sim **	*Diff **	*Sim **	*Diff **	W/m^3	A
			°C	°C	°C	°C	°C	°C	°C		
White	0.26	0.9	56.2	50	-1.4	25.12	-0.28	24.29	-0.11	242410	54.46
Grey	0.56	0.94	56.21	50	-1.3	25.11	+0.31	24.27	+0.57	242540	54.47
Black	0.97	0.91	56.2	50	-1.7	25.12	-1.38	24.28	-1.42	242440	54.46
White	0.26	0.9	62.35	55	-1.3	25.52	-0.38	24.52	-0.78	287310	59.29
Grey	0.56	0.94	62.36	55	-0.7	25.49	+1.39	24.5	+1.0	287450	59.3
Black	0.97	0.91	62.35	55	-1.4	25.51	-1.39	24.52	-1.48	287360	59.29
White	0.26	0.9	68.5	60	-1.1	25.91	+1.01	24.76	+1.26	332200	63.75
Grey	0.56	0.94	68.51	60	-0.6	25.88	+1.68	24.73	+1.23	332390	63.77
Black	0.97	0.91	68.5	60	-1.0	25.9	-0.9	24.75	-1.15	332250	63.76
White	0.26	0.9	74.65	65	-0.9	26.3	-0.6	25.0	-1.2	377100	67.92
Grey	0.56	0.94	74.66	65	-0.2	26.27	+1.47	24.97	+1.17	377310	67.94
Black	0.97	0.91	74.65	65	-0.8	26.29	-1.01	24.99	-1.31	377150	67.93
White	0.26	0.9	80.79	70	-0.9	26.69	-0.21	25.24	-0.66	421960	71.85
Grey	0.56	0.94	80.8	70	-0.3	26.66	+2.06	25.2	+1.6	422200	71.87
Black	0.97	0.91	80.8	70	-0.7	26.69	-0.41	25.23	-0.67	422070	71.86

* "Sim" denotes the simulated value, while "Diff" denotes the difference between the simulated and experimental values.

The thermal conductivities of all used materials are given in [4-6], while the radiation properties of pavement surfaces are outlined in Table III.

For the two cases relating to the large-size domain (Fig. 2), values for Q_v and I_{cp} are selected in such a manner so that they correspond to radiation properties of the acrylic black paint α=0.97 and ε=0.91, thermal conductivity of the concrete blocks k=1.3 W/(m·K) and continuously permissible temperature of the cable T_{cp}=90 °C, as follows: Q_v=448340 W/m^3 and I_{cp}=74.1 A – for the case I; and Q_v=445940 W/m^3 and I_{cp}=73.9 A – for the case II. The remaining input parameters are constant and can be found in [4]. The temperatures of the pavement, cable's outer surface and S-phase conductor which are obtained by simulations of the temperature distribution over the large-size domain are given in Table III.

Based on the results presented in Table III, it can be seen that the temperatures of the pavement, cable's outer surface and S-phase conductor decrease with decreasing the absorptivity-to-emissivity ratio α/ε. The same applies in both cases related to Fig. 2. This means it is possible to increase the ampacity by selecting a coating, paint or material with a lower value of the ratio α/ε. The phenomenon will be quantified later in this section. From Table III it can, also, be seen that the thermal effect of solar radiation increases by increasing the size of the cable bedding.

Fig. 3 presents the effect of the ratio α/ε on the temperature distribution over the part of the domain from Fig. 2 that represents the cable trench. It can be seen from these temperature distributions that, when the cool pavement with low α/ε ratio (according to [4-6], lower than 0.6) is applied, the temperature gradients within the cable, bedding and native soil are lower. This agrees with the observation derived from Table III. Hence, the heat is conducted in a more efficient manner from the cable to the cool pavement surface.

TABLE III. EFFECT OF PAVEMENT SURFACE RADIATION PROPERTIES ON TEMPERATURES OF PAVEMENT, CABLE'S OUTER SURFACE AND S-PHASE CONDUCTOR FOR THE CASES I AND II RELATING TO THE LARGE-SIZE DOMAIN IN FIG. 2

Material, coating or paint	Surface radiation property		Case I			Case II		
			Temperature			Temperature		
	Absorptivity, α	*Emissivity, ε*	*Pavement surface*	*Cable's outer surface*	*S-phase conductor*	*Pavement surface*	*Cable's outer surface*	*S-phase conductor*
	–	–	°C	°C	°C	°C	°C	°C
Cool white coating	0.15	0.9	20.5	52.5	64.1	21	50.8	62.3
Acrylic white paint	0.26	0.9	27.7	56.3	67.9	28.1	54.9	66.4
Concrete blocks	0.56	0.94	45	65.5	77	45.2	64.7	76.1
Asphalt	0.87	0.93	63.3	75.3	86.6	63.2	75.1	86.4
Acrylic black paint	0.97	0.91	69.7	78.7	90	69.5	78.8	90

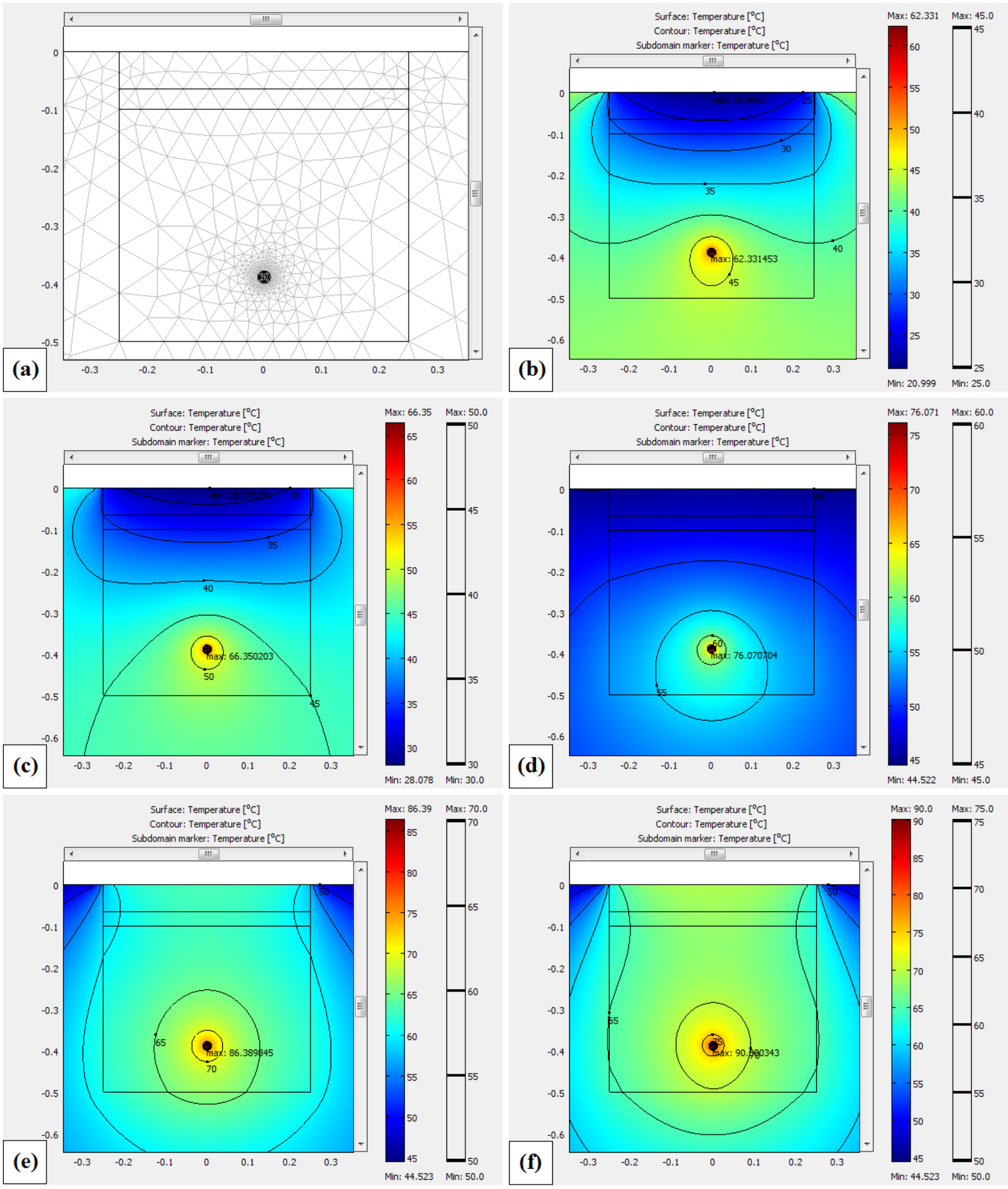

Figure 3. Temperature distribution over (a) the part of the computational domain from Fig. 2 that represents the cable trench, obtained for the case II when the upper surface of the trench is covered with (b) cool white coating, (c) acrylic white paint, (d) uncoated concrete blocks, (e) uncoated asphalt, and (f) acrylic black paint.

For the XP-00 4×16 mm^2 0.6/1 kV cable at reference operating conditions (laying depth 0.7 m, soil temperature at laying depth 20 °C and thermal conductivity of the soil 1 W/(m·K)), the ampacity making the temperature of the cable construction elements 90 °C equals 111 A [11]. The same ampacity can also be obtained numerically using the large-size model associated with Fig. 2 and a complete set of reference operating conditions. The complete set of reference operating conditions consisted of the following: laying depth 0.7 m, reference soil temperature 20 °C (at the boundaries positioned on the left-hand, right-hand and bottom side of the large-size domain), thermal conductivity of the native soil, cable bedding, backfill and pavement 1 W/(m·K), temperature of the air contacting the earth surface T_a=293.7 K, heat transfer coefficient due to convection

h=7.382 W/(m^2·K) obtained using the empirical correlation $h = 7.382 + 1.925 \cdot v_a^{0.75}$ for a wind velocity of v_a=0 m/s [4], thermal emissivity of the earth surface ε=0 and solar absorptivity of the earth surface α=0. Based on this FEM-based simulation, it is evident that the IEC-based procedure from [1] completely ignores the earth surface radiation properties and that the ampacity (I_{cp}=111 A) obtained for the standard reference operating conditions is about 1.5 times larger than the ampacities (I_{cp}=74.1 A and I_{cp}=73.9 A) obtained for the most unfavourable summer conditions.

Fig. 4 shows the temperatures of the S-phase conductor depending on the load current for laying depths of 0.4 m, 0.7 m and 1 m and for white, grey and black pavement surfaces. Fig. 4a corresponds to the case when the cable is laid in the bedding of size 0.5 m × 0.4 m, while Fig. 4b corresponds to the case when the trench is completely filled with bedding material.

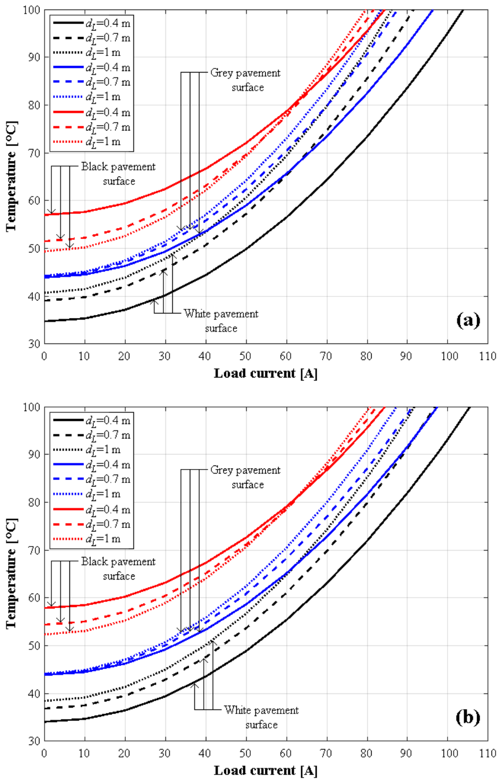

Figure 4. Temperature of the S-phase conductor versus load current for different laying depths and pavement surfaces: (a) bedding having dimensions 0.5 m × 0.4 m, and (b) trench completely filled with bedding material.

Figs. 4a and 4b show that the installation of the cable closer to the earth surface increases the load current for the white and grey pavement surfaces and decreases the load current for the black pavement surface. This applies to a temperature range up to about 81 °C. In the range from about 81 °C up to T_{cp}=90 °C, the installation of the cable closer to the earth surface increases the load current and ampacity for all three considered colors. For the temperatures up to about 81 °C, the results obtained for all three considered surfaces are in agreement with those reported in [4].

The ampacity values relating to a laying depth of 0.4 m and the white, grey and black pavement surfaces are, respectively, 95.7 A, 87.5 A and 74.1 A – according to Fig. 4a, and 97.2 A, 88.4 A and 73.9 A – according to Fig. 4b. When the cable is laid at a depth of 0.7 m, the ampacity values corresponding to the white, grey and black pavement surfaces are, respectively, 83.7 A, 79.4 A and 72.8 A – according to Fig. 4a, and 88.9 A, 82.7 A and 72.9 A – according to Fig. 4b. The ampacity values relating to the cable installed in the bedding of standard size at a depth of 1 m are 78.7 A, 75.8 A and 71.4 A for the white, grey and black pavement surfaces, respectively. When the cable is laid in the trench completely filled with bedding at a depth of 1 m, the ampacities corresponding to the white, grey and black pavement surfaces are 84 A, 79.2 A and 71.8 A, respectively. In addition, it can be observed that a completely filled trench does not contribute to the increase of cable ampacity only for the black pavement surface, because in this case the bedding material provides a better conductive path for the solar heat from the earth surface to the cable.

Standard procedures for calculation of the ampacity of underground cable lines do not take into consideration the effects of solar irradiance and earth surface radiation properties [1-3]. The effect of variation in solar irradiance on temperatures of underground cable conductors will be discussed in this and the next paragraph. Temperatures of the S-phase conductor are calculated for the different solar irradiances and white, grey and black pavement surfaces, at each of laying depths, by considering the load current values that make the temperature of the S-phase conductor 90 °C as constant value. As shown in Fig. 5, the decreasing solar irradiance contributes to the cooling of the S-phase conductor of the cable. In this case, the temperature of the S-phase conductor will reduce and there will be a significant increase in the ampacity. This applies to the other two phase conductors as well.

A value of 500 W/m^2 is taken as typical of the average solar irradiance on a clear day. By taking into account this solar irradiance and Fig. 5a, the temperature of the S-phase conductor of the cable installed in the bedding of standard size at depths of 0.4 m, 0.7 m and 1 m will decrease respectively by 13 °C, 14.3 °C and 14.7 °C – for the white pavement surface, 17.5 °C, 16.8 °C and 16.5 °C – for the grey pavement surface, and 23.3 °C, 20 °C and 18.7 °C – for the black pavement surface. These decreases for the cable installed in the bedding of standard size at depths of 0.4 m, 0.7 m and 1 m mean that the cable can respectively be loaded by 10.7 A, 11 A and 11 A – for the white pavement surface, 15.3 A, 13.4 A and 12.6 A – for the grey pavement surface, and 22.6 A, 16.9 A and 14.9 A – for the black pavement surface.

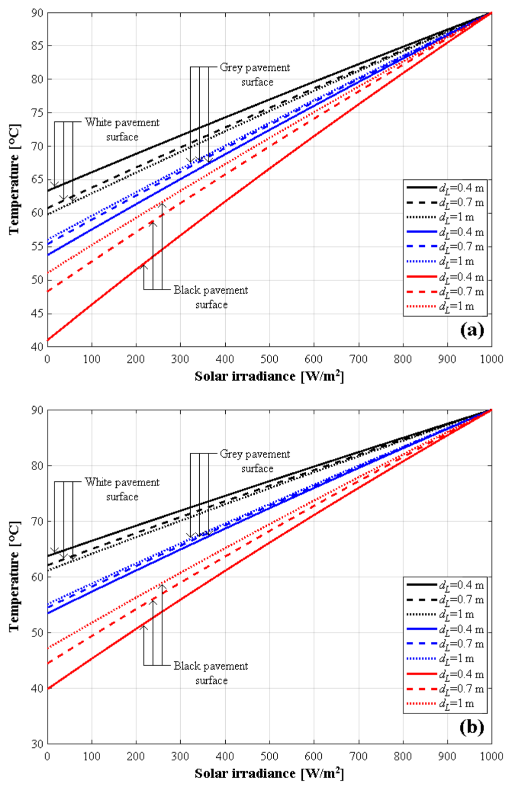

Figure 5. Temperature of the S-phase conductor versus solar irradiance for different laying depths and pavement surfaces: (a) bedding having dimensions 0.5 m × 0.4 m, and (b) trench completely filled with bedding material.

According to Fig. 5b, similar results are obtained when the cable trench is completely filled with bedding material. Therefore, it is clear that the installation of the cable closer to the earth surface increases the ampacity for the grey and black pavement surfaces. For the white pavement surface, the cable ampacity remains almost constant at 11 A.

In order to determine the cable ampacity I_{cp}, simulations of temperature distribution in the cases I and II at a depth of 0.7 m were performed with the most unfavourable summer conditions and the most common winter conditions, as well as with the radiation and thermal properties (α, ε and k) of the previously selected pavement surfaces and materials (Table III). The values for Q_v are gradually increased or decreased from arbitrary prescribed initial values to their values corresponding to T_{cp}=90 °C. Then, these values for Q_v and (2) are used to calculate the values of I_{cp}. The values of Q_v and I_{cp} are listed in Table IV.

Based on the quantification of the effects of the ratio α/ε and bedding size on the ampacity of the considered cable, the following can be observed: (i) In comparison with the black concrete-pavement, the other coated or uncoated surfaces can increase the ampacity up to 12.6 A – for the most unfavourable summer conditions and up to 5.2 A – for the most common winter conditions. (ii) The bedding having a size of 0.5 m × 0.735 m can additionally increase the ampacity up to 6 A – for the most unfavourable summer conditions and up to 5.6 A – for the most common winter conditions. Therefore, the ampacity can be increased by 18.6 A in summer and by 10.8 A in winter if the pavement is coated with cool white coating and if the trench is completely filled with the bedding material.

V. CONCLUSIONS

The conclusions that can be drawn from the presented results and discussion of them are:

- The simulated and experimental results are in good agreement.
- Compared to the corresponding cases with the black pavement, the ampacity of the considered cable laid at 0.7 m can be raised up to 25.6 % (or 18.6 A) in summer and up to 10.2 % (or 10.8 A) in winter. These results are obtained by taking into account the effects of the pavement surface radiation properties and bedding size.

TABLE IV. VOLUME POWERS OF HEAT SOURCES AND CABLE AMPACITIES CALCULATED FOR THE LAYING DEPTH OF 0.7 METERS AND DIFFERENT THERMAL ENVIRONMENTS IN SUMMER AND WINTER

Material, coating or paint	**Surface radiation property**	**Results obtained for the most unfavourable summer conditions**				**Results obtained for the most common winter conditions**			
		Case I		***Case II***		***Case I***		***Case II***	
	α/ε	Q_v	I_{cp}	Q_v	I_{cp}	Q_v	I_{cp}	Q_v	I_{cp}
	–	**W/m^3**	**A**	**W/m^3**	**A**	**W/m^3**	**A**	**W/m^3**	**A**
Cool white coating	0.167	596590	85.4	682240	91.4	1018540	111.6	1122160	117.2
Acrylic white paint	0.289	572850	83.7	646280	88.9	1005330	110.9	1102250	116.1
Concrete blocks	0.596	515480	79.4	559140	82.7	973160	109.1	1053800	113.5
Asphalt	0.935	454920	74.6	466640	75.6	937180	107.1	999100	110.6
Acrylic black paint	1.066	433540	72.8	433950	72.9	924500	106.4	980110	109.5

- The ampacity of the considered cable was found to increase with decreasing the absorptivity-to-emissivity ratio of the pavement surface, as well as with decreasing the laying depth of the cable (excluding the case of black pavement surface for the range up to about 81 °C).
- All the ampacity values obtained for the laying depth of 0.7 m and the most unfavourable summer conditions are lower than the reference value of 111 A. In addition, for the most common winter conditions, the ampacity values are lower or greater, by 4.6-6.2 amperes, than the reference value of 111 A.
- From the point of view of the solar irradiance, the ampacity of the considered cable increases with decreasing the laying depth in the case of grey or black pavement surface, and stays almost constant with decreasing the laying depth in the case of white pavement surface.
- The results obtained for the XLPE-cable changes according to a law similar to that observed in [4] for a PVC-cable. This should be further investigated in one of the next studies.

ACKNOWLEDGMENT

This paper was based on research conducted within the project TR33046 funded by the Ministry of Education, Science, and Technological Development of the Republic of Serbia.

REFERENCES

[1] International Electrotechnical Commission, IEC 60287-1-1:2006+AMD1:2014 CSV, Electric Cables – Calculation of the Current Rating – Part 1-1: Current Rating Equations (100% Load Factor) and Calculation of Losses – General, 2.1 edition, Geneva, Switzerland, 2014.

[2] International Electrotechnical Commission, IEC TR 62095:2003, Electric cables – Calculations for current ratings – Finite element method, 1st edition, Geneva, Switzerland, 2003.

[3] National Fire Protection Association, NFPA 70, National Electrical Code, 2017 Edition, Quincy, MA, USA, 2016.

[4] D. Klimenta, B. Perović, J. Klimenta, M. Jevtić, M. Milovanović, I. Krstić, "Modelling the thermal effect of solar radiation on the ampacity of a low voltage underground cable," International Journal of Thermal Sciences, Vol. 134, 2018, pp. 507–516.

[5] D. Klimenta, B. Perović, J. Klimenta, M. Jevtić, M. Milovanović, I. Krstić, "Controlling the thermal environment of underground cable lines using the pavement surface radiation properties," IET Generation, Transmission & Distribution, Vol. 12, Issue 12, 2018, pp. 2968–2976.

[6] D. O. Klimenta, B. D. Perović, J. Lj. Klimenta, M. M. Jevtić, M. J. Milovanović, I. D. Krstić, "Controlling the thermal environment of underground power cables adjacent to heating pipeline using the pavement surface radiation properties," Thermal Science, Vol. 22, No. 6A, 2018, pp. 1–16.

[7] L. Lindström, "Evaluating impact on ampacity according to IEC-60287 regarding thermally unfavourable placement of power cables," Masters' Degree Project, Royal Institute of Technology (KTH), Stockholm, Sweden, November 2011, XR-EE-ETK 2011:009.

[8] J. Nahman, M. Tanaskovic, "Calculation of the ampacity of high voltage cables by accounting for radiation and solar heating effects using FEM," International Transactions on Electrical Energy Systems, Vol. 23, Issue 3, 2013, pp. 301–314.

[9] J. Nahman, M. Tanaskovic, "Evaluation of the loading capacity of a pair of three-phase high voltage cable systems using the finite-element method," Electric Power Systems Research, Vol. 81, Issue 7, 2011, pp. 1550–1555.

[10] J. Nahman, M. Tanaskovic, "Calculation of the loading capacity of high voltage cables laid in close proximity to heat pipelines using iterative finite-element method," International Journal of Electrical Power and Energy Systems, Vol. 103, 2018, pp. 310–316.

[11] L. Heinhold, Power Cables and their Application – Part 1, third revised ed., Siemens Aktiengesellschaft, Berlin and Munich, Germany, 1990.